International Journal of Heat and Fluid Flow 31 (2010) 83–92

Contents lists available at ScienceDirect

International Journal of Heat and Fluid Flow

journal homepage: www.elsevier.com/locate/ijhff

# Modelling of combined surface radiation and natural convection in a vented "T" form cavity

Ahmed Mezrhab [a,*], Samir Amraqui [a], Chérifa Abid [b]

[a] Université Mohammed 1[er], Faculté des Sciences, Département de Physique, Laboratoire de Mécanique et Energétique, 60000 Oujda, Morocco
[b] Université d'Aix-Marseille 1, Polytech' marseille, IUSTI CNRS 6595, Technopole Château Gombert, 5 Rue Enrico Fermi, 13453 Marseille Cedex 13, France

ARTICLE INFO

*Article history:*
Received 31 October 2008
Received in revised form 6 September 2009
Accepted 14 October 2009
Available online 22 November 2009

*Keywords:*
Heat transfer
Isothermal blocks
Natural convection
Surface radiation
"T" form cavity

ABSTRACT

In this paper, a numerical study of heat transfer and fluid flow in a "T" form cavity is carried out. The cavity contains two symmetrically identical isothermal blocks and is vented by two opening located in a vertical median axis at the top and the bottom parts of the cavity. A specifically developed numerical model, based on the finite-volume method, is used for the solutions of the governing differential-equations. The coupling of the velocity–pressure is treated by the Simpler algorithm. A special attention is given to study the effects of block height, opening size, Rayleigh number and surface emissivity of blocks and walls. Effects of different parameters on streamlines, temperature fields and average Nusselt-number are discussed. It is found that the radiative exchanges produce an increase of the average Nusselt-number. This one increases almost linearly with increasing the Rayleigh number *Ra*, and it becomes more important when the solid blocks heights are large.



## 1. Introduction

Enhancement of the heat transfer by natural convection in the geometry of a cavity has been extensively studied numerically and experimentally because of its interest and importance in engineering designs and related problems, such as solar collector, thermal insulation, cooling of electronic components and building design (e.g., Kelkar and Patankar, 1990; Karayiannis et al., 1992; Khan and Yao, 1993; Nag et al., 1994; Sun and Emery, 1994). Natural convection in a cavity fitted with an array of rectangular blocks on either the top or bottom wall has also attracted a lot of attention. Hasnaoui et al. (1990) have numerically studied the effect of buoyancy on the flow and heat transfer that develop between a horizontal cold surface and an infinite two-dimensional array of open cavities heated from below. Because of the periodicity of the geometry and boundary conditions, the numerical calculations were restricted to a simple representative domain. It was shown that, depending on the values attributed to the governing geometric and thermophysical parameters, the final flow state achieved may be stationary, periodic or chaotic. Also, it was found that the relative height of the adiabatic blocks has a strong effect on the transition from steady state solutions to periodic ones and on the destruction of the flow symmetry. Amahmid et al. (1997) carried out a numerical study about an infinite horizontal channel containing an indefinite number of uniformly spaced rectangular, heated and isothermal blocks. They studied the effect of the computational domain choice on the multiplicity of solutions. The effect of each solution on the flow and the heat transfer is examined. Their investigations show that the symmetry of the flow is not always maintained although the boundary conditions for this problem are symmetrical.

Recently, Kwak and Song (2000) conducted experimental and numerical studies of natural convection heat transfer from vertical plates with horizontal rectangular grooves. They studied the effect of Rayleigh number for each aspect ratio of the considered system. They found, for given conditions, secondary recirculation flows in the grooves and they established a proper correlation to obtain the heat transfer rate from each pitch for the given geometries and Rayleigh numbers. In an other work, Bilen et al. (2001) made an experimental and numerical study about the effect of the position of wall mounted rectangular blocks on the heat transfer from the surface, taking into account the angular displacement of the block in addition to its spanwise and streamwise disposition. In their experiments, the effect of variable parameters (distance between adjacent blocks, block displacement angle and Reynolds number) was examined. The results showed that the most efficient parameters were Reynolds number and angular disposition. The distance between blocks has a slightly increasing effect on the heat transfer. Desrayaud and Fichera (2002) studied numerically the natural convection in a vertical channel obstructed by two symmetrical isothermal or adiabatic ribs. They found that the best position of the ribs for heat extraction depends on the magnitude of the Rayleigh number. Moreover, the increase of the rib length has

* Corresponding author.
*E-mail address:* mezrhab@fso.ump.ma (A. Mezrhab).

0142-727X/$ - see front matter © 2009 Elsevier Inc. All rights reserved.
doi:10.1016/j.ijheatfluidflow.2009.10.004

**Nomenclature**

| | |
|---|---|
| $A_i$ | radiative surface number $i$ |
| $d$ | distance between two adjacent blocks, m |
| $D$ | dimensionless distance between two blocks, $d/L$ |
| $F_{i-j}$ | view factor between $A_i$ and $A_j$ |
| $G$ | gravity acceleration, m s$^{-2}$ |
| $h$ | height of the blocks, m |
| $H$ | dimensionless heigth of the blocks, $h/L$ |
| $K$ | thermal conductivity, W m$^{-1}$ K$^{-1}$ |
| $l_o$ | opening size, m |
| $L$ | cavity length, m |
| $L_o$ | dimensionless opening size, $l_o/L$ |
| $N$ | total number of radiative surfaces |
| $Nr$ | radiation number, $\sigma T_h^4/(k\Delta T/L)$ |
| $Nu$ | average Nusselt-number |
| $P$ | dimensional pressure, Pa |
| $P$ | dimensionless pressure, $(p+\rho_0 gy)L^2/\rho_0\alpha$ |
| $Pr$ | Prandtl number, $\nu/\alpha$ |
| $Q$ | throughflow strength |
| $Ra$ | Rayleigh number, $g\beta(T_h-T_c)L^3/\nu\alpha$ |
| $R_i$ | dimensionless radiosity of surface $A_i$ |
| $T$ | temperature, K |
| $T_0$ | average temperature, $(T_h+T_c)/2$, K |
| $u,v$ | velocity components, m s$^{-1}$ |
| $U,V$ | dimensionless velocity components, $U=uL/\alpha$, $V=vL/\alpha$ |
| $x, y$ | coordinates Cartesian, m |
| $X,Y$ | dimensionless coordinates, $X = x/L$, $Y = y/L$ |

*Greek symbols*

| | |
|---|---|
| $\delta_{ij}$ | Kronecker symbol |
| $\alpha$ | thermal diffusivity of the fluid, m$^2$ s$^{-1}$ |
| $\beta$ | volumetric expansion coefficient, K$^{-1}$ |
| $\Delta T$ | maximal difference temperature, $(T_h-T_c)$, K |
| $\varepsilon_i$ | emissivity of surface $A_i$ |
| $\varphi_r$ | radiative flux density, W m$^{-2}$ |
| $\phi_r$ | dimensionless radiative flux density, $\phi_r/\sigma T_h^4$ |
| $\nu$ | kinematic viscosity of the fluid, m$^2$ s$^{-1}$ |
| $\rho_0$ | density of the fluid at $T_0$, kg m$^{-3}$ |
| $\Theta$ | dimensionless temperature, $T/T_h$ |
| $\theta$ | dimensionless temperature, $(T-T_c)/\Delta T$ |
| $\sigma$ | Stefan–Boltzmann constant, W K$^{-4}$ m$^{-2}$ |

*Subscripts*

| | |
|---|---|
| $c$ | cold |
| $f$ | fluid |
| $h$ | hot |
| $o$ | opening |
| $w$ | wall |
| $b$ | block |

only a limited influence on the heat transfer while the increase of its width decreases dramatically the mass flow rate and the heat transfer especially when the region obstructed was greater than the half of the opening.

More recently, a numerical investigation was conducted by Najam et al. (2002, 2003) to study the enhancement of heat transfer in a cavity with heated rectangular blocks and submitted to a vertical jet of fresh air from below. Because of the problem periodicity, the calculation domain is reduced to a "T" form cavity. El Alami et al. (2004) studied the chimney effect by natural convection from an obstructed vented cavity. They demonstrated that: the apparition of recirculations cells is due to the amplification of heat transfer by the increase of the Rayleigh number, the average Nusselt-number increases considerably with the solid block height and the correlation obtained for the average Nusselt-number is similar to that obtained in the case of the blocked chimneys.

Few studies have treated the coupling between surface radiation and natural convection. Among these works, we quote the one of Balaji and Venkateshan (1994) who have reported the numerical results of the fundamental problem of interaction of surface radiation with free convection in an open cavity with air as the intervening medium. Rayleigh numbers (based on height) in the laminar range $10^4$–$10^8$ have been considered in their numerical study. It was found that the surface radiation alters the basic flow pattern as well as overall thermal performance of the open cavity. Balaji and Venkateshan (1995) carried out a detailed numerical study of conjugate natural convection with surface radiation from a slot (closed end open cavity) where both the vertical walls were conducting and the bottom wall was isothermal. Various Rayleigh numbers, thermal conductivities, emissivity and aspect ratios were considered, while conducting the parametric study. A correlation was given for the average Nusselt-number by taking into account all the pertinent parameters.

Research interests in this field are continuous. Han and Baek (2000) numerically studied natural convection of a radiating fluid in a rectangular enclosure, with two incomplete adiabatic thin partitions (one on the top and the other at the bottom) under a large temperature difference. They have used the finite-volume method (FVM) to solve the radiative transport equation, and have found that the radiation alters significantly the flow patterns and the thermal distributions. In addition, the surface radiation was dominant over the gas radiation and the results were affected by the baffle configuration. The effects of both surface radiation and gaseous radiation were considered; however he concluded that the predominant mechanism by which the radiation process will increase the overall heat transfer rates is the surface radiation. Ramesh and Merzkirch (2001) made an experimental study of the combined natural convection and thermal radiation heat transfer in a cavity with top opening. They found that the surface thermal radiation heat transfer in cavities with wall of high emissivity has a significant change in the flow and temperature patterns. Singh and Venkateshan (2004) discussed a numerical study of combined laminar natural convection and surface radiation heat transfer in a 2D side vented open cavity for different aspect ratio, side-vent ratios and surface emissivity using air as the working fluid. Based on numerical data separate average Nusselt-number correlations have been developed for convective and radiative heat transfer. Mezrhab et al. (2005) presented a numerical study, based on a finite-volume method and a boundary element approximation, of the radiation–natural convection interactions in a differentially heated square enclosure, within which a centered, squared, heat-conducting body generates heat. They found that the streamlines and isotherms structures in the enclosure are strongly affected by the thermal radiation heat transfer. Moreover, this one increases considerably the total heat transfer in the enclosure, and allows a good cooling of the body that generates heat. Finally, Mezrhab et al. (2006) have numerically studied the radiation–natural convection interactions in a vertical vented chimney. The chimney is divided, in its center, by a thin partition. The study shows that the thermal radiation increases considerably the heat transfer within the chimney and that the position and the size influence of the additional opening is significant only in the presence of the radiative exchanges.

The objective of the present investigation is to study numerically the surface radiation effect on the heat transfer and the air flow in a "T" form cavity with heated rectangular blocks. In comparison to the previous works achieved on the "T" form cavity, the originality of our contribution consists in the taking into account of the surface radiation in this kind of geometry.

## 2. Mathematical modelling and analysis

### 2.1. Description of the physical model

Schematic of the problem with coordinate system and boundary conditions is presented in Fig. 1. It shows the geometry of a "T" form cavity with identical rectangular blocks of height $h$ and width $L$ placed on its lower wall. To allow a vertical ventilation of the system, two coaxial openings are added at the level of the horizontal rigid boundaries. The blocks are heated at a constant temperature $T_h$, and connected with adiabatic surfaces. The upper wall of the cavity is maintained at a cold temperature $T_c$.

The flow is assumed to be incompressible, laminar and two-dimensional in a square "T" form cavity. The fluid under study is air and its physical properties are assumed to be constant at the average temperature $T_0$ except for density whose variation with the temperature is allowed in the buoyancy term. The walls of the cavity and the blocks are grey diffuse emitters and reflectors of radiation.

### 2.2. Mathematical modelling

The dimensionless form of the governing equations can be obtained by introducing the dimensionless variables. These are defined as follows:

$$X = x/L; \quad Y = y/L$$
$$U = uL/\alpha; \quad V = vL/\alpha$$
$$\theta = (T - Tc)/(Th - Tc); \quad P = (p + \rho g y)L^2/\rho_0\alpha^2$$

Variables $u$, $v$ and $T$ are the velocity components in the $x$, $y$ direction and temperature, respectively. Quantities $\rho_0$ and $\alpha$ are the density and the thermal diffusivity of the fluid at $T_0$, respectively. Based on the dimensionless variables above, the dimensionless equations for the conservation of mass, momentum, and energy equations are:

$$^{*}\text{Continuity}: \quad \frac{\partial U}{\partial X} + \frac{\partial V}{\partial Y} = 0 \tag{1}$$

$$^{*}X\text{-momentum}: \quad U\frac{\partial U}{\partial X} + V\frac{\partial U}{\partial Y} = -\frac{\partial P}{\partial X} + Pr\left(\frac{\partial^2 U}{\partial X^2} + \frac{\partial^2 U}{\partial Y^2}\right) \tag{2}$$

$$^{*}Y\text{-momentum}: \quad U\frac{\partial V}{\partial X} + V\frac{\partial V}{\partial Y} = -\frac{\partial P}{\partial Y} + Pr\left(\frac{\partial^2 V}{\partial X^2} + \frac{\partial^2 V}{\partial Y^2}\right) + Ra\,Pr\,\theta \tag{3}$$

$$^{*}\text{Energy}: \quad U\frac{\partial \theta}{\partial X} + V\frac{\partial \theta}{\partial Y} = \left(\frac{\partial^2 \theta}{\partial X^2} + \frac{\partial^2 \theta}{\partial Y^2}\right) \tag{4}$$

Hot and cold walls are maintained at dimensionless temperature of 1 and 0, respectively.

Symmetry conditions have been employed on the left and right boundaries of the computational domain. The relevant boundary conditions are:

$$X = 0.25 \text{ and } 0 \leqslant Y \leqslant H: \quad U = V = 0, \;\; \theta = 1 \tag{5}$$
$$X = 0.75 \text{ and } 0 \leqslant Y \leqslant H: \quad U = V = 0, \;\; \theta = 1 \tag{6}$$
$$X = 0 \text{ and } H \leqslant Y \leqslant 1: \quad U = V = 0, \;\; \frac{\partial \theta}{\partial X} - Nr\phi_r = 0 \tag{7}$$
$$X = 1 \text{ and } H \leqslant Y \leqslant 1: \quad U = V = 0, \;\; \frac{\partial \theta}{\partial X} - Nr\phi_r = 0 \tag{8}$$
$$Y = H \text{ and } 0 \leqslant X \leqslant 0.25: \quad U = V = 0, \;\; \theta = 1 \tag{9}$$
$$Y = H \text{ and } 0.75 \leqslant X \leqslant 1: \quad U = V = 0, \;\; \theta = 1 \tag{10}$$

$$Y = 0 \text{ and } \frac{1}{2} - \frac{L_0}{2} \leqslant X \leqslant \frac{1}{2} + \frac{L_0}{2}: \quad U = 0, \quad \frac{\partial V}{\partial Y} = 0, \;\; \theta = 0, \;\; P = -\frac{Q_{in}^2}{2} \tag{11}$$

$$Y = 0 \text{ and } \left(X < \frac{1}{2} - \frac{L_0}{2} \text{ or } X > \frac{1}{2} + \frac{L_0}{2}\right): \quad U = V = 0, \;\; \frac{\partial \theta}{\partial Y} - Nr\phi_r = 0 \tag{12}$$

$$Y = 1 \text{ and } \left(\frac{1}{2} - \frac{L_0}{2} \leqslant X \leqslant \frac{1}{2} + \frac{L_0}{2}\right): \quad U = 0, \;\; \frac{\partial V}{\partial Y} = 0, \;\; \frac{\partial \theta}{\partial Y} = 0, \;\; P = 0 \tag{13}$$

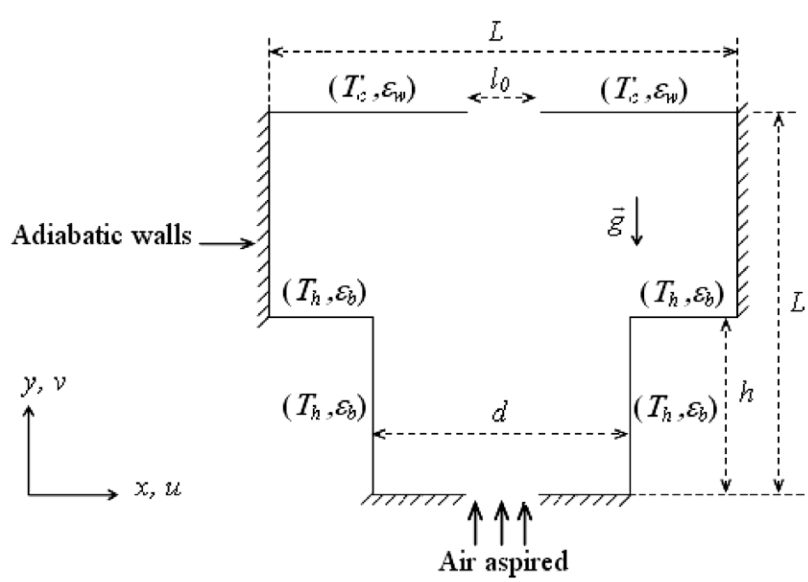


**Fig. 1.** Schematic drawing of the physical model.

$$Y = 1 \text{ and } \left(X < \frac{1}{2} - \frac{L_0}{2} \text{ or } X > \frac{1}{2} + \frac{L_0}{2}\right): \quad U = V = 0, \quad \theta = 0 \tag{14}$$

where $Q_{in}$ is given by:

$$Q_{in} = \int_{\frac{1}{2}-\frac{L_0}{2}}^{\frac{1}{2}+\frac{L_0}{2}} [V(X)]_{Y=0} dX \tag{15}$$

### 2.3. Coupling radiation and natural convection

For the radiative heat transfer problem, the working fluid (air) is considered to be perfectly transparent. Thus, the air does not participate to the radiative heat transfer, and only the solid surfaces contribute to the radiation exchange. These one are assumed to be diffuse-grey. In this case, indeed, one knows that the radiative transfers appear in the heat balance of the system only on the level of the boundary conditions. Thus, after having established the boundary conditions, which describe the radiative exchanges between surfaces, the problem is to evaluate the radiative heat flux, which comes in the expression of the assessment of energy at the border of the solid node. The walls of the cavity and blocks boundaries are divided into finite number of zones on which the four basic assumptions of the simplified zone analysis were assumed valid. The number of zones retained was determined by the mesh used to solve the differential-equations.

The coupling of the thermal model is performed by computing the radiative exchanges. The determination of the net radiative flux density requires the knowledge of the surface temperature of each node. Writing the thermal balance of each surface provides us with these temperatures.

A balance between radiation, conduction and convection determines the thermal condition at the surface of the plate:

$$R_k \frac{\partial \theta_s}{\partial n} = \frac{\partial \theta}{\partial n} - Nr\phi_r \tag{16}$$

where $n$ denotes the unit normal direction to the surface at the solid–air interface and $\phi_r$ is the dimensionless net radiative flux density along this surface.

For the insulated wall, the Eq. (16) becomes:

$$\frac{\partial \theta}{\partial n} - Nr\phi_r = 0 \tag{17}$$

Therefore, the dimensionless net radiative flux density along a diffuse grey and opaque surface $A_i$ ($i$ = 1, $N$) is expressed as:

$$\phi_{r,i} = R_i - \sum_{j=1}^{N} R_j F_{i-j} \tag{18}$$

where $N$ is the number of total radiative surfaces. The dimensionless radiosity is obtained by resolving the following system:

$$\sum_{j=1}^{N} (\delta_{ij} - (1 - \varepsilon_i)F_{i-j})R_j = \varepsilon_i \Theta_i^4 \tag{19}$$

The average Nusselt-number $Nu$, which is of a greater interest in engineering applications, is used to provide an idea on the heat transfer characteristics. In this problem, it is composed of the convective and radiative Nusselt-numbers.

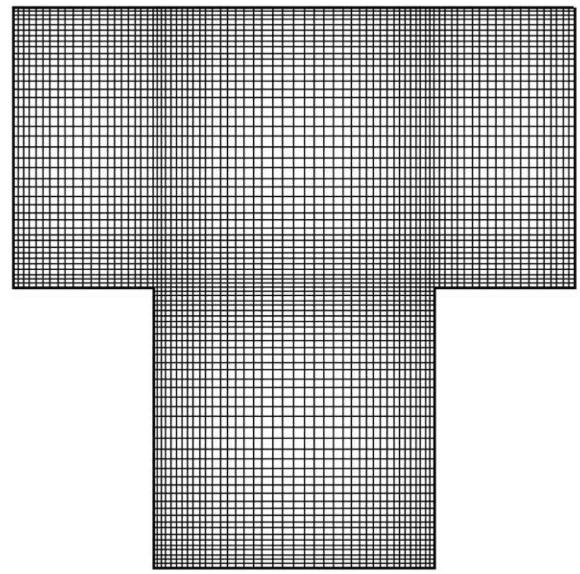

**Fig. 2.** Schematic presentation of the grid.

$$Nu = Nur + Nuc \tag{20}$$

where $Nuc$ and $Nur$ are the convective and radiative contributions in $Nu$. They are given by:

$$Nuc = 2\left[\frac{1}{H}\int_0^H \left(-\frac{\partial \theta}{\partial X}|_{(X_w=0.25,Y)}\right)dY + \frac{1}{0.25}\int_0^{0.25}\left(-\frac{\partial \theta}{\partial Y}|_{(X,Y_w=H)}\right)dX\right] \tag{21}$$

$$Nur = 2\left[\frac{1}{H}\int_0^H (N_r\phi_r(X_w = 0.25, Y)dY + \frac{1}{0.25}\int_0^{0.25} (N_r\phi_r(X, Y_w = H)dX\right] \tag{22}$$

### 2.4. Numerical technique

Numerical solutions of Eqs. (1)–(4) were obtained by using a finite-volume method utilizing a second order central difference scheme (CDS) for the advective terms. The pressure–velocity coupling is assured by the SIMPLER (Semi-Implicit Method for Pressure Linked Equations Revised) algorithm (Patankar, 1980). The iterative process is repeated until steady state: max $|\phi^{(n+1)} - \phi^{(n)}| < \varepsilon_\phi$ where $\phi$ is a dependent variable and $n$ is the iteration number. In this study, the velocity components and temperature were driven to $\varepsilon_u = \_v = \varepsilon_\theta < 10^{-6}$ and for pressure $\varepsilon_p < 10^{-8}$. The resulting systems of discretized equations were solved by a conjugate gradient method.

**Table 1**
Grid independence study (natural convection combined to the surface radiation case: $\varepsilon$ = 1).

| $Ra$ | Size | $Nu$ | $\psi_{max}$ | Q |
|---|---|---|---|---|
| $10^5$ | 40 × 40 | 25.6118 | 21.3695 | 23.669 |
| | 60 × 60 | 26.7468 | 22.8612 | 24.563 |
| | 80 × 80 | 26.8492 | 23.8915 | 24.865 |
| | 100 × 100 | 26.8521 | 23.8944 | 24.911 |
| | 120 × 120 | 26.8681 | 23.9634 | 25.008 |

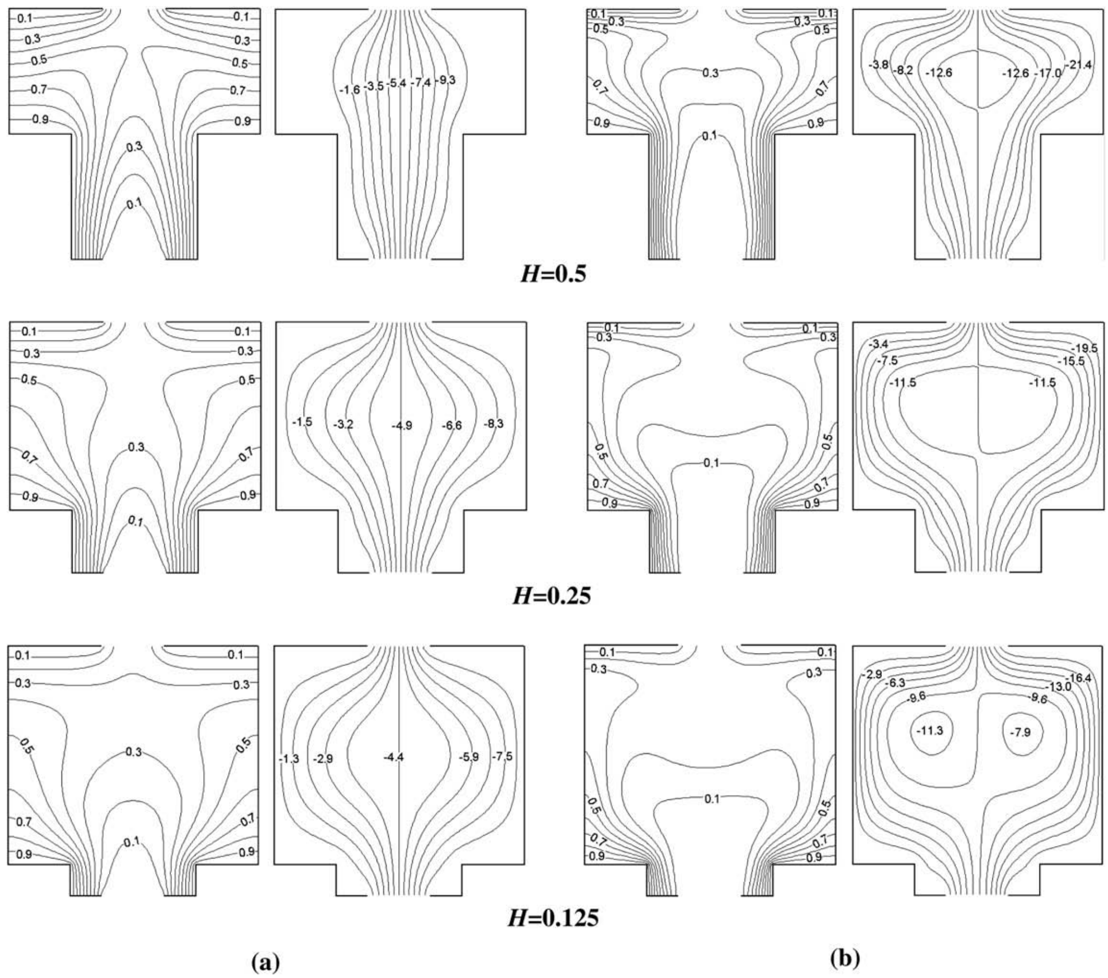


**Fig. 3.** Effect of the height of the blocks on the isotherms and the streamlines for $\varepsilon = 0$: (a) $Ra = 10^4$ and (b) $Ra = 10^5$.

Eq. (16) is non-linear owing to the net radiative flux, which is a function of $\theta_i^4$. It is solved with an iterative procedure at every time step for the energy equation (Eq. (4)). The surface temperatures were updated from the solution of the energy equation by under-relaxing the boundary evaluation of temperature. At each inner iteration, the linear system of equations for the radiosities (Eq. (19)) is solved by a direct method (Gauss elimination).

The grid was constructed such that the boundaries of physical domain coincided with the velocity grid lines. The points for pressure and temperature were placed at the center of the scalar volumes. At the interfaces fluid–solid, the control volume faces were also arranged so that a control volume face coincided with an interface. This grid distribution was chosen to ensure the interface energy balance. To avoid a check-board pressure and velocity fields, staggered grids were used for the $U$ and $V$-velocity components in the $X$ and $Y$-directions respectively.

Since the radiative properties of the solid surfaces of the enclosure vary from point (even on the isothermal side walls because the inside radiation cannot be assumed as uniform), each of the surfaces was divided into finite number of zones on which the four basic assumptions of the simplified zone analysis was assumed valid. The number of radiative surfaces retained was determined by the mesh used to solve the differential-equations. For $N$ control volume faces, this results in $N(N-1)/2$ view factors to be calculated and in a linear system of $N$ equations for the radiosities. The view factors were determined by using a boundary element approximation to fit the surfaces and a Monte Carlo method for the numerical integrations (Mezrhab and Bouzidi, 2005).

## 3. Grid size sensitivity

In order to ensure the grid-independence solutions, series of trial calculation were conducted for different grid distributions: $40 \times 40$; $60 \times 60$; $80 \times 80$; $100 \times 100$; $120 \times 120$. Table 1 presents a comparison of the predicted average Nusselt-numbers, the maximum stream function and the mass flow rate using different grid arrangements, in pure natural convection combined to the surface radiation case for $Ra = 1 \times 10^5$, $H = D = 0.5$ and $L_o = 0.25$. It was observed that difference between the results of the grid $80 \times 80$ and those of the grid $120 \times 120$ are of 0.07% for the average Nusselt-number, 0.30% for the maximum stream function and 0.57% for the mass flow rate. Consequently, to optimize appropriate grid refinement with computational efficiency, the grid $80 \times 80$ was chosen for all the further computations. The grid is non-uniform and fine near the solid surfaces (Fig. 2).

## 4. Results and discussion

The code was extensively exercised on benchmark problems to check its validity. In the cases of an empty cavity, a square cavity with a solid block, the results that we obtain with our simulation technique were checked for accuracy against the earlier published

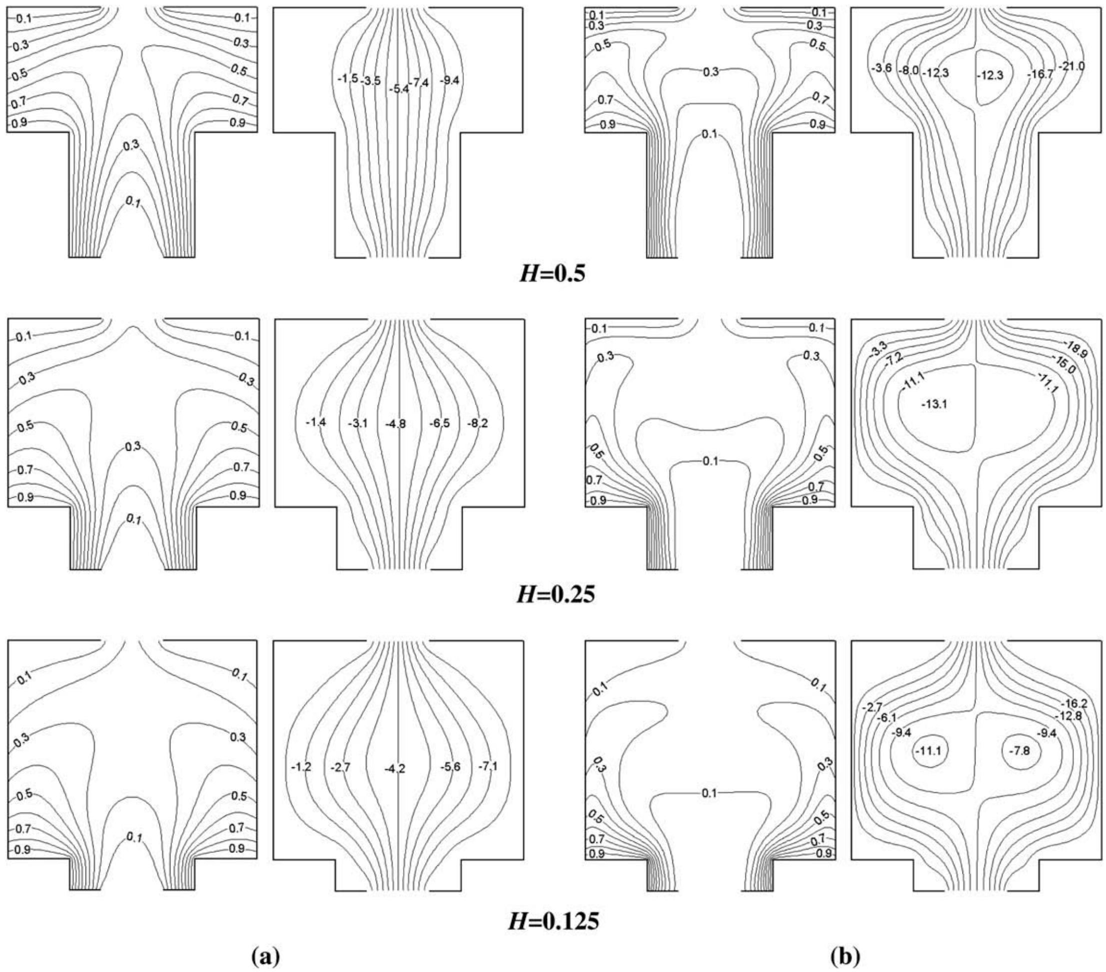


**Fig. 4.** Effect of height blocks on the isotherms and the streamlines for Fig. 4. Effect of the height of the blocks on isotherms and streamlines for $\varepsilon = 1$: (a) $Ra = 10^4$ and (b) $Ra = 10^5$.

numerical and experimental results reported by different authors, and the agreement between the present and previous results was very good in Ref. (Mezrhab et al., 2006). The code was also validated for vertical channels divided by a partition as shown in Ref. (Bouali and Mezrhab, 2006). It was concluded that the largest discrepancies between our and published results can be estimated to be less than 1%. For this reason and for the sake of brevity it is not repeated here. Based on the above mentioned studies, it was concluded that the code could be reliably applied to the problem considered here.

The mathematical model developed in the last section was used to investigate the pure natural convection and natural convection coupled with surface radiation. Each case required the specification of five dimensionless parameters ($Pr$, $Ra$, $H$, $L_o$, $\varepsilon$) among which the Prandtl number is fixed to $Pr = 0.71$. On the other hand, the same emissivity $\varepsilon$ is chosen of all radiative surfaces, except when its effect is investigated. In cases where we do not investigate the effects of surface emissivity, this one is noted simply $\varepsilon$ and is equal to 1 in presence of the radiation exchange and 0 otherwise. The remaining parameters have been varied with the aim of studying their effects on the heat transfer and the air flow in the cavity. In this study, $T_0$ is chosen equal to 300 K, and in order to keep available the Boussinesq approximation ($\Delta T < 0.1T_h$) (Zhong et al., 1985), the terminal temperature difference $\Delta T$ is kept equal to 20 K. Hence, $T_h$ and $T_c$ are fixed to 310 K and 290 K, respectively. When one holds into account the radiation exchange, the characteristic dimension $L$

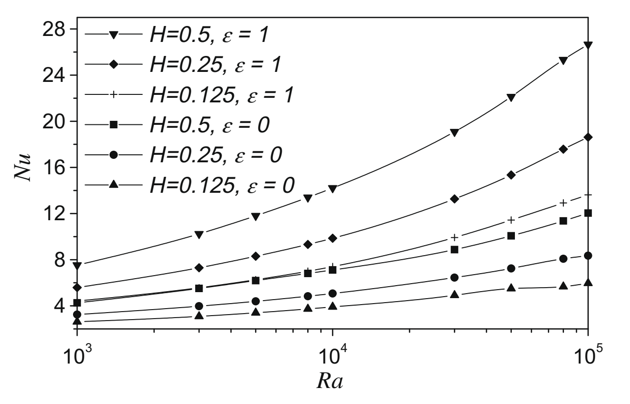


**Fig. 5.** The radiation effect and the heigth of the blocks on the average Nusselt-number.

of the "T" form cavity is calculated according to the Rayleigh number and is used to determine the radiation number $Nr$.

### 4.1. Effect of the blocks height

The effects caused by the variation of the solid block height, on the isotherms and streamlines in absence (Fig. 3) and in presence (Fig. 4) of the surface radiation, are presented for $L_o = 0.25$, $D = 0.5$

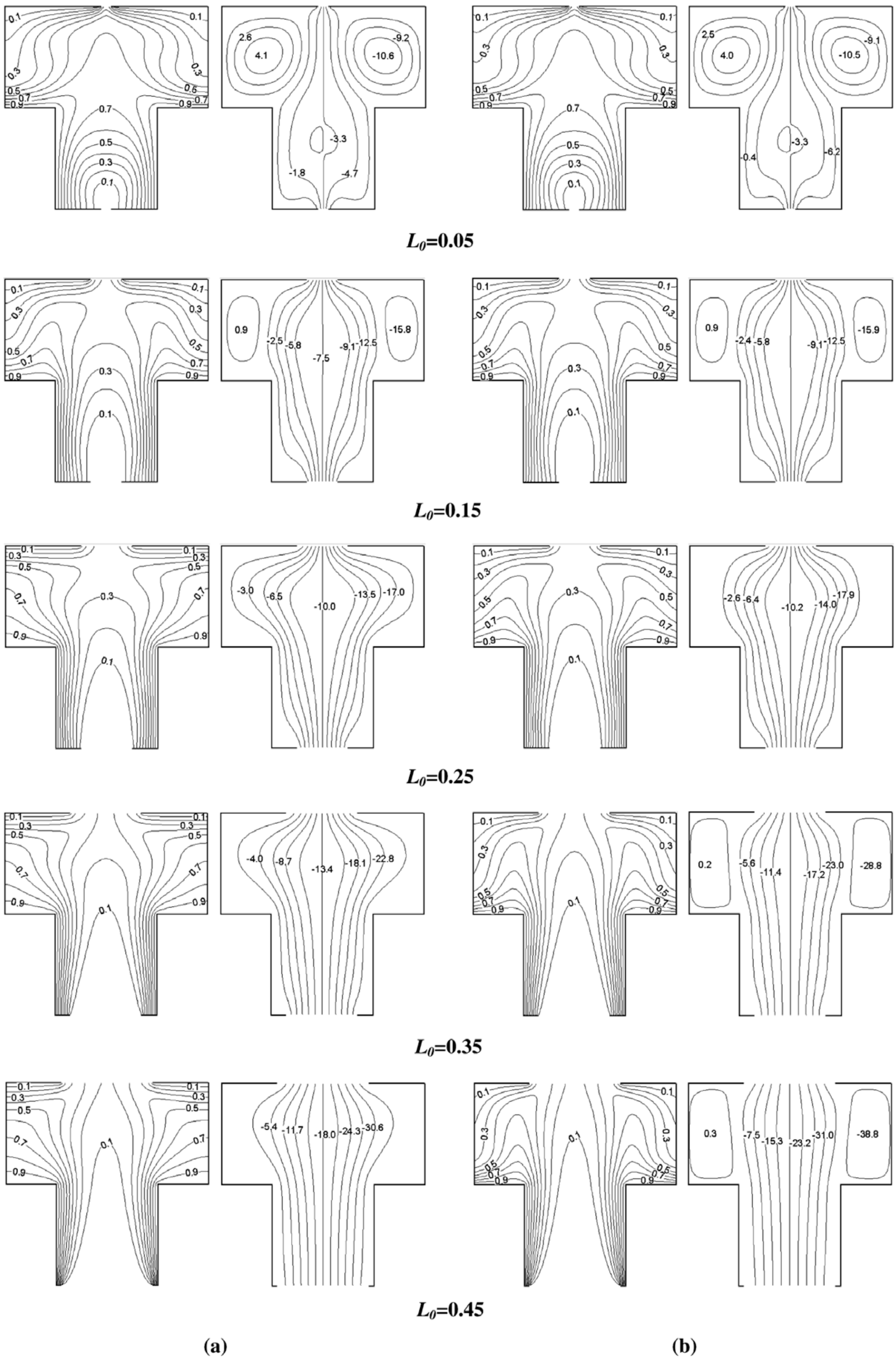


**Fig. 6.** Opening size effect on isotherms and steamlines for $Ra = 5 \times 10^4$: (a) $\varepsilon = 0$ and (b) $\varepsilon = 1$.

and for two Rayleigh numbers $Ra = 10^4$ and $10^5$. The three heights of solid blocks, selected in this study are: $H = 0.5$, $H = 0.25$ and $H = 0.125$. These figures also allow us to analyze the surface radiation effect on the isotherms and the streamlines shape.

Let us note that for all cases, the isotherms and the streamlines are symmetric with respect to the vertical median of the cavity. Independently of the value of $H$, we can see that the air circulation increases with increasing the Rayleigh number $Ra$. In fact, the air aspired by the chimney effect at the inlet opening increases under the effects of the buoyancy forces which are due to the increase of $Ra$.

In the pure natural convection ($\varepsilon = 0$) and for $Ra = 10^4$, it is noted that when the solid block height is large ($H = 0.5$), the flow is stagnant in the left and right parts of the upper half of the "T" form cavity. That is explained by the fact that the flow is channelled around the central vertical axis of the cavity. For this height and for $Ra = 10^5$, we note the increase of the air circulation in the entire cavity owing to the increase of the buoyancy forces. In this case, the isotherms are concentrated close to the hot and cold walls indicating a more important heat transfer from the hot isothermal walls towards the remainder of the cavity.

When the solid block height $H$ decreases from $H = 0.5$ to $H = 0.125$, the air circulation decreases. This can be explained by the fact that the height of the two hot walls is reduced which causes a decrease in the chimney effect and consequently produces a decrease in the mass flow rate of the air aspired at the opening inlet.

When $H = 0.5$, the isotherms are concentrated near the cold and hot walls compared to the case where $H$ is smaller. This means that the heat transfer is important when $H$ is large. This remark is confirmed by Fig. 4 representing the height effect $H$ of the solid block on the average Nusselt-number.

In the natural convection mode combined to the surface radiation ($\varepsilon = 1$, Fig. 4), the isotherms structure in the regions close to the adiabatic walls is due to the importance of the radiative fluxes. In fact in this case, the isotherms are tilted close to the adiabatic walls whereas they are perpendicular in pure natural convection. Moreover, the inclination of the isotherms is more important when $Ra$ is large. This is explained by the fact that the radiation number $Nr$ is proportional to $Ra$. The streamlines show that the surface radiation causes a considerably increase of the air circulation in the "T" form cavity. It is clear that the length effect of the solid blocks on the isotherms and streamlines structures, especially in the cavity center is similar to that noted in the pure natural convection case.

Fig. 5 shows the variation of the average Nusselt-number $Nu$ according to the Rayleigh number in presence and in absence of the radiation exchange and for three heights of the blocks $H = 0.125$, 0.25 and 0.5. In a general way, the average Nusselt-number $Nu$ increases with the Rayleigh number $Ra$, because of the effects of the natural convection and the surface radiation which are more significant for larges $Ra$ values. It should be noted that the average Nusselt-number increases with increasing the solid block height; particularly when the emissivity of solid surfaces is equal to 1. This is means that the chimney effect is more pronounced when the solid block height is large; especially in presence of the surface radiation.

### 4.2. Opening size effect

Fig. 6 presents the isotherms and streamlines for five opening size with ($\varepsilon = 1$) and without ($\varepsilon = 0$) the radiation exchange, respectively at $\Delta T$=20 K, $Ra = 5 \times 10^4$ and $H = D = 0.5$. It is clear that the vent opening size affects strongly the isotherms and streamlines structures inside the "T" form cavity, especially in the left and right sides of the upper half of the cavity. Owing to the air entering from the opening, the density of streamlines increases just upstream of the opening, what yields to the increase of the isotherms density in the same region.

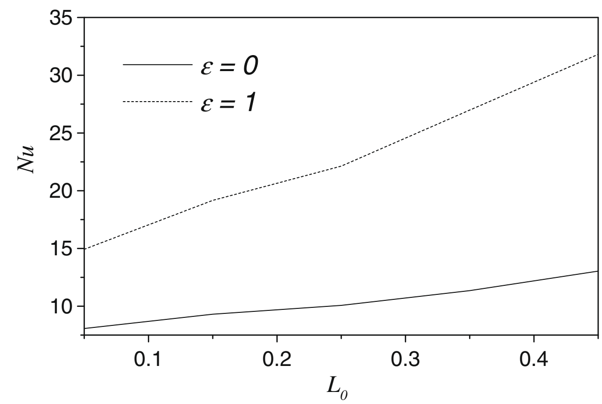


**Fig. 7.** The average Nusselt versus the opening size for $Ra = 5 \times 10^4$.

The effect of the opening size $L_o$ on the average Nusselt-number $Nu$, in presence ($\varepsilon = 1$) and in absence ($\varepsilon = 0$) of the radiation exchange, is shown in Fig. 7. As can be seen, it is clear that the average Nusselt-number increases with $L_o$. The enhancement of heat transfer in a heated "T" form cavity containing two opening located at the top and bottom can be explained by the conduction effects because of restricted air flows and a chimney effect that must be responsible for the increase in convective heat transfers. In presence of the radiation exchange, $Nu$ evolves in the same way but it increases in value.

### 4.3. Surface emissivity effects

Fig. 8 depicts the isotherms and streamlines for $Ra = 5 \times 10^4$, $H = D = 0.5$, $L_o = 0.25$ and $\Delta T$=20 K according to the block emissivity for two extreme values of the wall emissivity ($\varepsilon_w = 0.25$ and 1). For a fixed wall emissivity, the effect of thermal radiation becomes important with the increase of the block emissivity. On the other hand, the radiation exchange effect is more pronounced for large values of the block and wall emissivities. Note that the inclination of the isotherms near the insulated wall is clearly seen even at low values of the block and walls emissivities. However, the inclination at the insulated walls becomes remarkable only for large values of the wall emissivity.

Figs. 9 and 10 show respectively the average radiative and convective Nusselt-numbers according to the wall emissivity $\varepsilon_w$, with the block emissivity $\varepsilon_b$ as a curve parameter. $Ra$, $H$, $D$, $L_o$, and $\Delta T$ are fixed to $5 \times 10^4$, 0.5, 0.5, 0.25 and 20 K, respectively.

For a non-zero surface emissivity $\varepsilon_b$, Fig. 9 shows that the average radiative Nusselt-number $Nur$ decreases with increasing $\varepsilon_w$. As $\varepsilon_b$ increases, $Nur$ becomes larger and decreases slightly with increasing $\varepsilon_w$. The rate of a decrease in the value of $Nur$ with $\varepsilon_w$ is more important for low values of $\varepsilon_b$. In fact, the radiative Nusselt-number is governed by $\phi_r$ as indicated in Eq. (22) since $Nr$ is constant because it depends only upon $Ra$, $T_0$ and $\Delta T$ which are fixed. Moreover, $\phi_r$ depends upon the emissivities of the block $\varepsilon_b$ and the enclosure walls $\varepsilon_w$; and it decreases with decreasing $\varepsilon_b$ and/or increasing $\varepsilon_w$.

Fig. 10 shows that the increase of $\varepsilon_w$ causes an increase in the average convective Nusselt-number $Nuc$ for any value of $\varepsilon_b$. The rate of increase in the value of $Nuc$ with $\varepsilon_w$ is more important as $\varepsilon_b$ approaches its minimum value ($\varepsilon_b = 0$). The increase of the average convective Nusselt-number according to the wall emissivity is explained by the fact that the temperature of the walls increases according to the wall emissivity, causing an increase of the convective Nusselt-number since the air temperature, licking the walls, is cold. For a fixed value $\varepsilon_w$, the average convective Nusselt-number

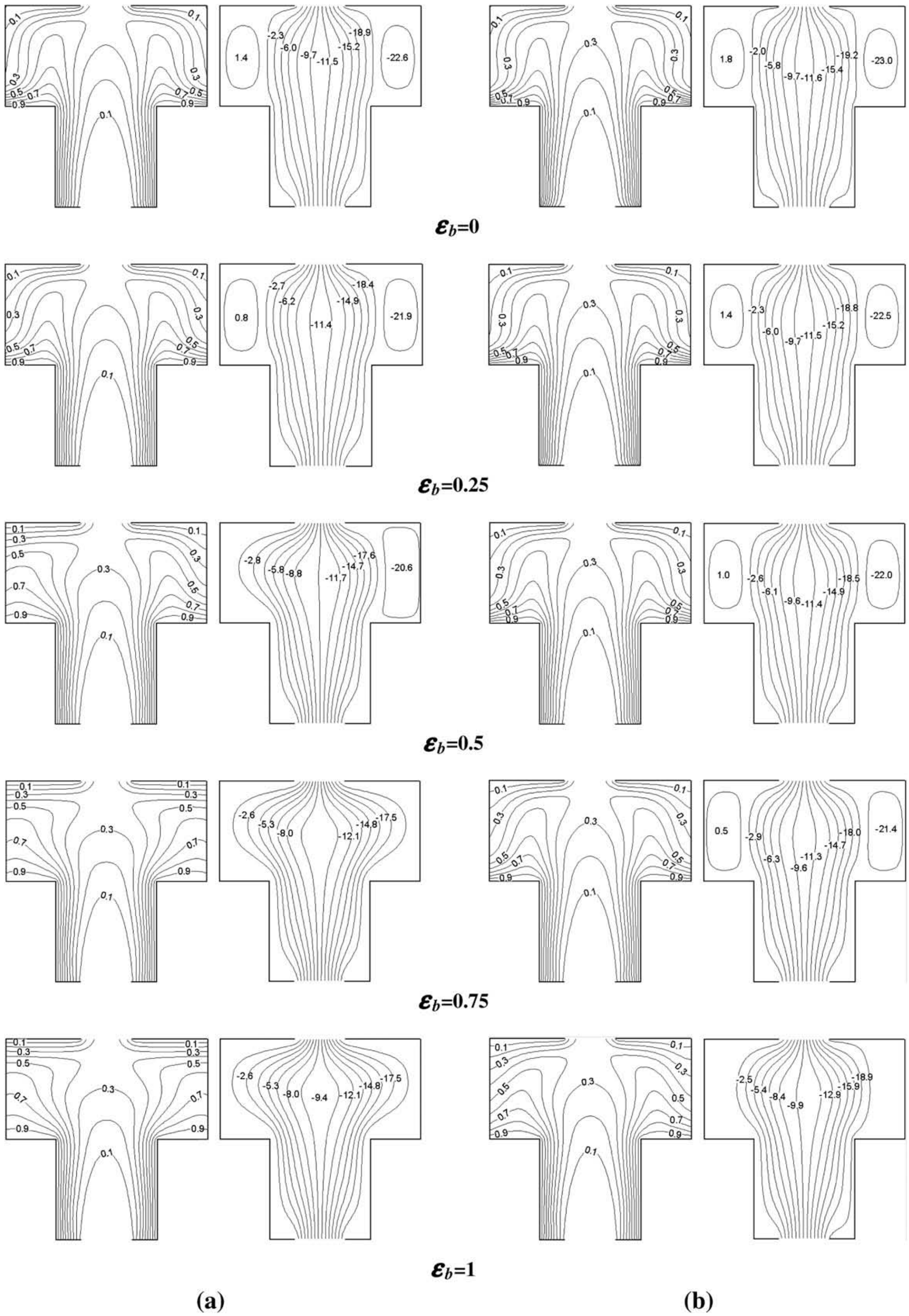


**Fig. 8.** Effect of surface emissivity on the isotherms and the streamlines for $Ra = 5 \times 10^4$: (a) $\varepsilon_w = 0.25$ and (b) $\varepsilon_w = 1$.

*Nuc* increases with decreasing the surface emissivity $\varepsilon_b$. In fact, when the block emissivity is lower, the air entering in the cavity is less heated which explains a greater convective transfer between the air and the hot blocks. From the streamlines pattern, it can be seen that for a fixed $\varepsilon_w$, the air velocity near the walls increases as the block emissivity decreases.

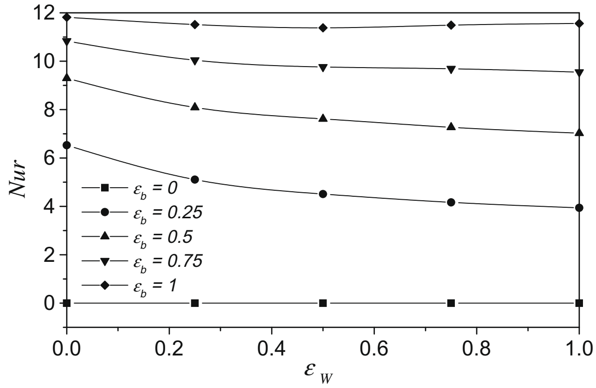


**Fig. 9.** The average radiative Nusselt-number for $Ra = 5 \times 10^4$.

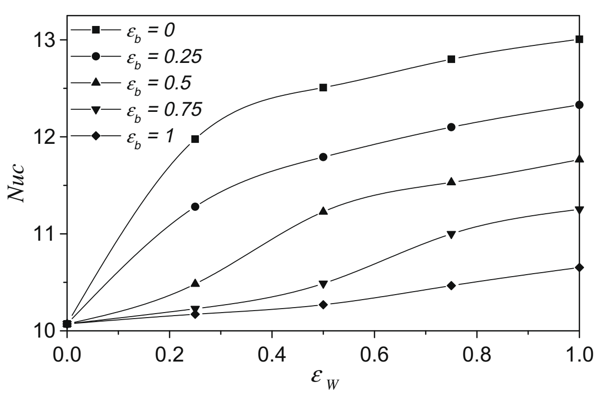


**Fig. 10.** The average convective Nusselt-number for $Ra = 5 \times 10^4$.

## 5. Conclusions

In this study we showed the effects of the solid blocks height, the opening size, the Rayleigh number and the surface emissivity of blocks and enclosure walls on the heat transfer and the air flow in a "T" form cavity. The principal conclusions obtained lead to:

(1) The surface radiation affects the isotherms and the streamlines structure, and causes a considerable increase of the heat transfer through the "T" form cavity. These effects are increasingly important as *Ra* increases.
(2) The solid blocks height *H* modifies the isotherms and streamlines appearance in the "T" form cavity. The air circulation decreases with decreasing *H* and the isotherms are concentrated near the isothermal walls when $H = 0.5$ compared to the case where *H* is smaller. The average Nusselt-number increases with increasing *H*, especially in presence of the surface radiation.
(3) The opening size affects the streamlines and isotherms structures inside the "T" form cavity, particularly at and above the region occupied by the opening. The density of streamlines increases just upstream of the opening, what yields to the increase of the isotherms density in the same region. The average Nusselt-number increases with increasing the opening size $L_o$. This increase is more important in presence of the radiation exchange.
(4) The emissivities of the enclosure walls and the blocks cause a considerably change in the thermal fields. For a constant value $\varepsilon_w$, the average Nusselt-number *Nuc* (*Nur*) increases (decreases) with decreasing the surface emissivity $\varepsilon_b$.

## References

Amahmid, A., Hasnaoui, M., Vasseur, P., 1997. Multiplicity of solutions in natural convection under a repetitive geometry. International Journal of Heat and Mass Transfer 40 (16), 3805–3818.
Balaji, C., Venkateshan, S.P., 1994. Interaction of radiation with free convection in an open cavity. International Journal of Heat and Fluid Flow 15, 317–324.
Balaji, C., Venkateshan, S.P., 1995. Combined conduction, convection and radiation in a slot, cavity. International Journal of Heat and Fluid Flow 14, 260–267.
Bilen, K., Yapici, S., Celik, C., Taguchi, A., 2001. Approach for investigation of heat transfer from a surface equipped with rectangular blocks. Energy Conversion and Management 42, 951–961.
Bouali, H., Mezrhab, A., 2006. Combined convective and radiative heat transfer in a divided channel. International Journal of Numerical Methods for Heat and Fluid Flow 16 (1), 84–106.
Desrayaud, G., Fichera, A., 2002. Laminar natural convection in a vertical isothermal channel with symmetric surface mounted rectangular ribs. International Journal of Heat and Fluid Flow 23, 519–529.
El Alami, M., Najam, M., Semma, E., Oubarra, A., Penot, F., 2004. Chimney effect in a "T" form cavity with heated isothermal blocks: the blocks height effect. Energy Conversion and Management 45, 3181–3191.
Han, C.Y., Baek, S.W., 2000. The effects of radiation on natural convection in a rectangular enclosure divided by two partitions. Numerical Heat Transfer Part A 37, 249–270.
Hasnaoui, M., Bilgen, E., Vasseur, P., 1990. Natural convection above an array of open cavities heated from below. Numerical Heat Transfer Part A 18, 463–482.
Karayiannis, T.G., Ciofalo, M., Barbaro, G., 1992. On natural convection in a single and two zone rectangular enclosure. International Journal of Heat and Mass Transfer 105, 89–95.
Kelkar, K.M., Patankar, S.V., 1990. Numerical prediction of natural convection in square partitioned enclosures. Numerical Heat Transfer Part A 17, 269–285.
Khan, J.A., Yao, G.F., 1993. Comparison of natural convection of water and air in a partitioned rectangular enclosure. International Journal of Heat and Mass Transfer 36 (12), 3107–3117.
Kwak, C.E., Song, T.H., 2000. Natural convection around horizontal downward-facing plate with rectangular grooves: experiments and numerical simulations. International Journal of Heat and Mass Transfer 43, 825–838.
Mezrhab, A., Bouali, H., Abid, C., 2005. Modelling of combined radiative and convective heat transfer in an enclosure with a heat-generating conducting body. International Journal of Computational Methods 2 (3), 431–450.
Mezrhab, A., Bouali, H., Amaoui, H., Abid, C., 2006a. Natural convection-radiation cooling of a vertical divided vented channel. Engineering Computations: International Journal for Computer-Aided Engineering and Software 23 (7), 818–839.
Mezrhab, A., Bouali, H., Amaoui, H., Bouzidi, M., 2006b. Computation of combined natural convection and radiation heat transfer in a cavity having a square body at its center. Applied Energy 83, 1004–1023.
Mezrhab, A., Bouzidi, M., 2005. Computation of view factors for surfaces of complex shape including screening effects and using a boundary element. Engineering Computations: International Journal for Computer-aided Engineering and Software 22 (2), 132–148.
Nag, A., Sarkar, A., Sastri, V.M.K., 1994. Effect of a thick horizontal partial-partition attached to one of the active walls of a differentially-heated square cavity. Numerical Heat Transfer Part A 25, 611–625.
Najam, M., El Alami, M., Hasnaoui, M., Amahmid, A., 2002. Numerical study of mixed convection in a "T" form cavity submitted to constant heat flux and ventilated from below with a vertical jet. CR Mécanique 330, 461–467.
Najam, M., El Alami, M., Oubarra, A., 2003. Heat transfer in a "T" form cavity with heated rectangular blocks submitted to a vertical jet: the block gap effect on multiple solutions. Energy Conversion and Management 45 (1), 113–125.
Patankar, S.V., 1980. Numerical Heat Transfer and Fluid Flow. Hemi-sphere, New York.
Ramesh, N., Merzkirch, W., 2001. Combined convective and radiative heat transfer in side-vented pen cavity. International Journal of Heat and Fluid Flow 22, 180–187.
Singh, S.N., Venkateshan, S.P., 2004. Numerical study of natural convection with surface radiation in side-vented open cavities. International Journal of Thermal Sciences 43, 865–876.
Sun, Y.S., Emery, A.F., 1994. Multigrid computation of natural convection in enclosures with a conductive baffe. Numerical Heat Transfer Part A 25, 575–592.
Zhong, Z.Y., Yang, K.T., Lloyd, J.R., 1985. Variable property effects in laminar natural convection in a square enclosure. Journal of Heat Transfer 17, 133–138.